Supplementary Information (SI) for Journal of Materials Chemistry A.

Supporting Information

A Simple Surface Engineering Approach to Enhance the Schottky Barrier of Polymer Dielectrics for Superior Energy Storage Performance

Tao Liu,[a] Yang Liu,[a] Jin Qian,[b] Jiajia Ren,[a] Jiwei Zhai,*[b] Tao Zhou,*[c] Yao Zhou,[d] Gui-Wei Yan,[a] Di-Ming Xu,[a] Wenfeng Liu,*[d] and Di Zhou*[a]

[a]Electronic Materials Research Laboratory & Multifunctional Materials and Structures, Key Laboratory of the Ministry of Education & International Center for Dielectric Research, School of Electronic Science and Engineering, Xi'an Jiaotong University, Xi'an, Shaanxi 710049, China

[b]Functional Materials Research Laboratory, School of Materials Science and Engineering, Tongji University, Shanghai, 201804, China.

[c]School of Electronic and Information Engineering, Hangzhou Dianzi University, Hangzhou, Zhejiang, China (Tao Zhou, zhou.tao@hdu.edu.cn)

[d]State Key Laboratory of Electrical Insulation and Power Equipment, Xi'an Jiaotong University, Xi'an 710049, Shaanxi, China.

---

* Corresponding author: Di Zhou (zhoudi1220@xjtu.edu.cn)
* Corresponding author: Jiwei Zhai (apzhai@tongji.edu.cn)
* Corresponding author: Tao Zhou (zhou.tao@hdu.edu.cn)
* Corresponding author: Wenfeng Liu (liuwenfeng@mail.xjtu.edu.cn)

Experimental Section

Materials

SiO_2 nanoparticles with an average particle size of 30 nm and N, N-dimethylformamide (DMF) were purchased from Shanghai Aladdin Biochemical Technology Co. P(VDF-HFP) particles were supplied by Polyk Technologies, USA. The PET film (9.8 μm) was provided by Anhui Tongfeng Electronics Co.

Preparation of SiO_2-Coated PET Films

To prepare the coating precursor, 0.5 g of P(VDF-HFP) particles, dried at 60 °C for 24 hours, are added to 10 mL of DMF. The mixture is magnetically stirred at 800 rpm for 4 hours at 30 °C to obtain a P(VDF-HFP)/DMF solution. Subsequently, SiO_2 nanoparticles, also dried at 60 °C for 24 hours, are introduced into 10 mL of DMF and subjected to tip sonication for 3 hours to yield a SiO_2/DMF solution. The SiO_2/DMF solution is then added to the P(VDF-HFP)/DMF solution under stirring and is magnetically stirred at 800 rpm for 8 hours at room temperature to ensure uniform dispersion of SiO_2.

PET polymer films, after being cleaned with ethanol, are immersed in the coating precursor solution for 1 minute. To achieve a uniform coating on the substrate surface, the coating process is repeated twice. Following coating, the films are vertically suspended in an oven and dried at 60 °C for 12 hours.

Characterizations

The micro-morphology of the polymer films was characterized by field emission scanning electron microscopy (SEM, FEI Quanta 250FEG). The structural properties of the films were analyzed by X-ray diffractometer (XRD, Rigaku D/MAX-2400). Absorption spectra of the polymer films were obtained using a UV-Vis spectrophotometer (PE Lambda950, China) and were used to calculate the energy band widths of the polymer dielectrics. The surface potential of the samples was characterized using a Kelvin probe force microscope (KPFM, SPM-9700HT, Japan). The high temperature dielectric properties were tested by a precision LCR bridge (E4980A, Agilent, USA) at a ramp rate of 3 °C/min. The frequency dependence of the dielectric properties was evaluated by a precision impedance analyzer (E4990A, Agilent, USA) at room temperature. The DC resistivity and breakdown voltage of the composites at different temperatures were measured using a high resistance meter (HP4339A, Agilent) and a dielectric breakdown tester (RK2671AM), respectively. TSDC was tested using a Keithley 6517B electrostatic meter. Leakage currents and D-E hysteresis loops were tested using a ferroelectric test system (aix ACCT, TF Analyzer 2000, Germany). Charge-discharge tests at different temperatures were performed with a high-voltage charge-discharge test system (CF-003, Shanghai Tongguo Intelligent Technology Co., Ltd.).

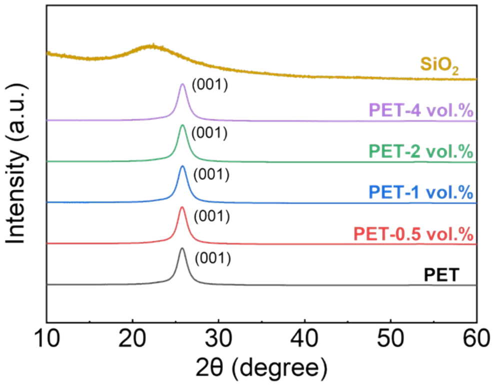

Figure S1. XRD spectrum of the PET-S films.

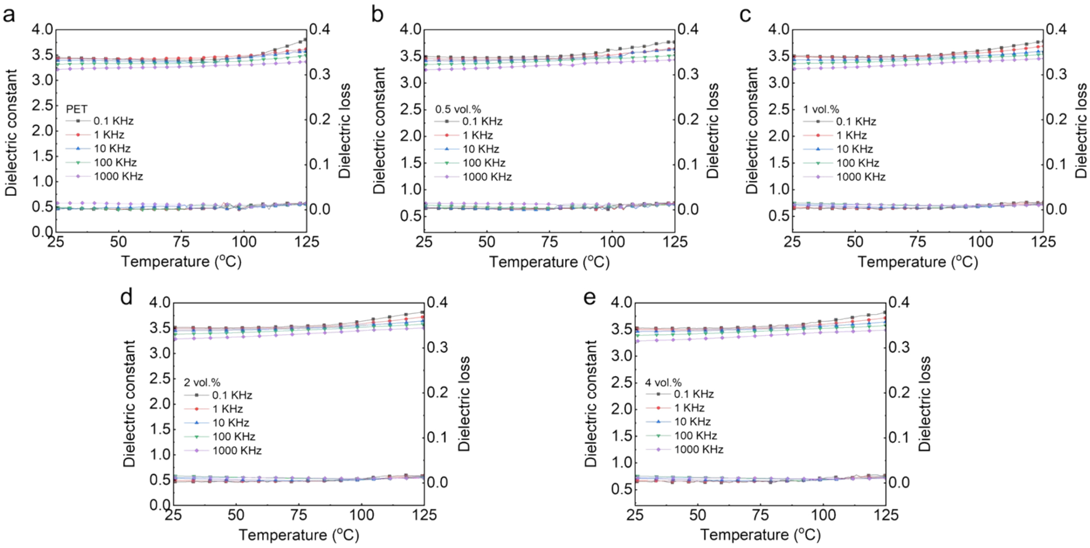

Figure S2. Variation in dielectric constant and dielectric loss of the PET-S films at different frequencies and specific temperatures.

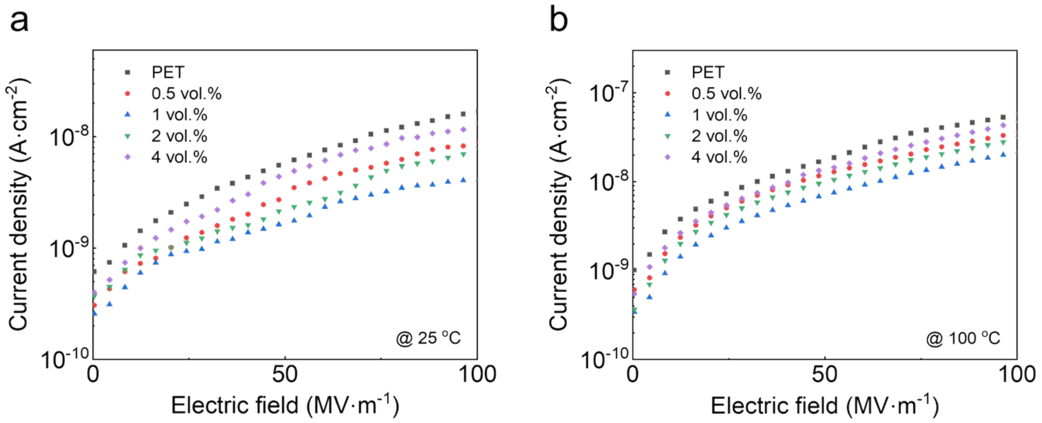

Figure S3. Variation of leakage current density with applied electric field for PET-S films at different temperatures: (a) 25 °C. (b) 100 °C.

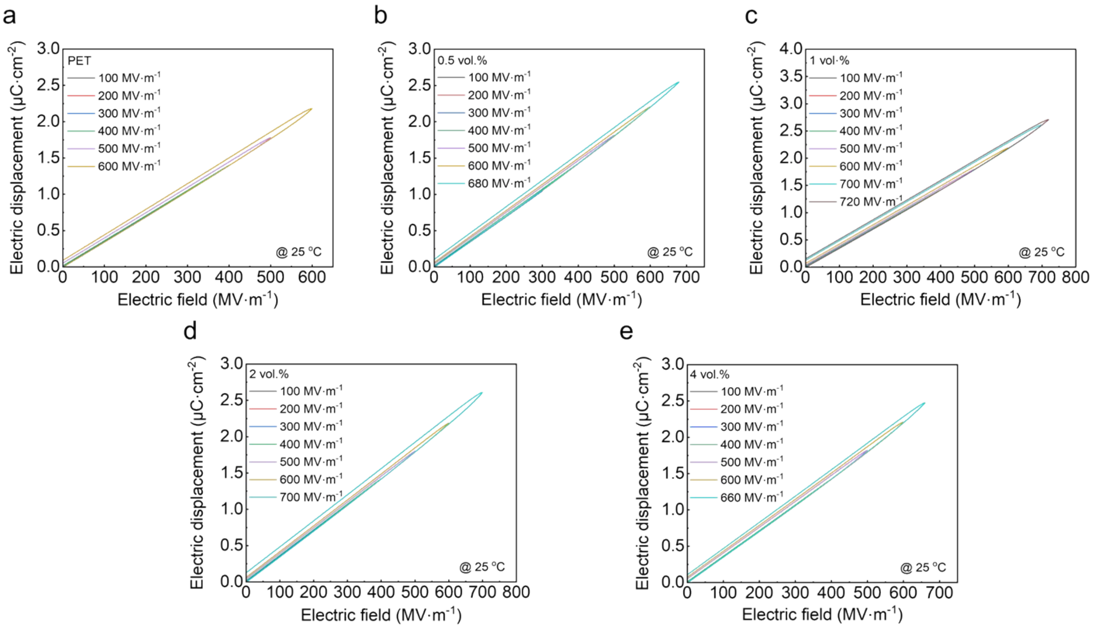

Figure S4. D-E hysteresis loops of PET and PET-S films at 25 °C under different electric field strengths.

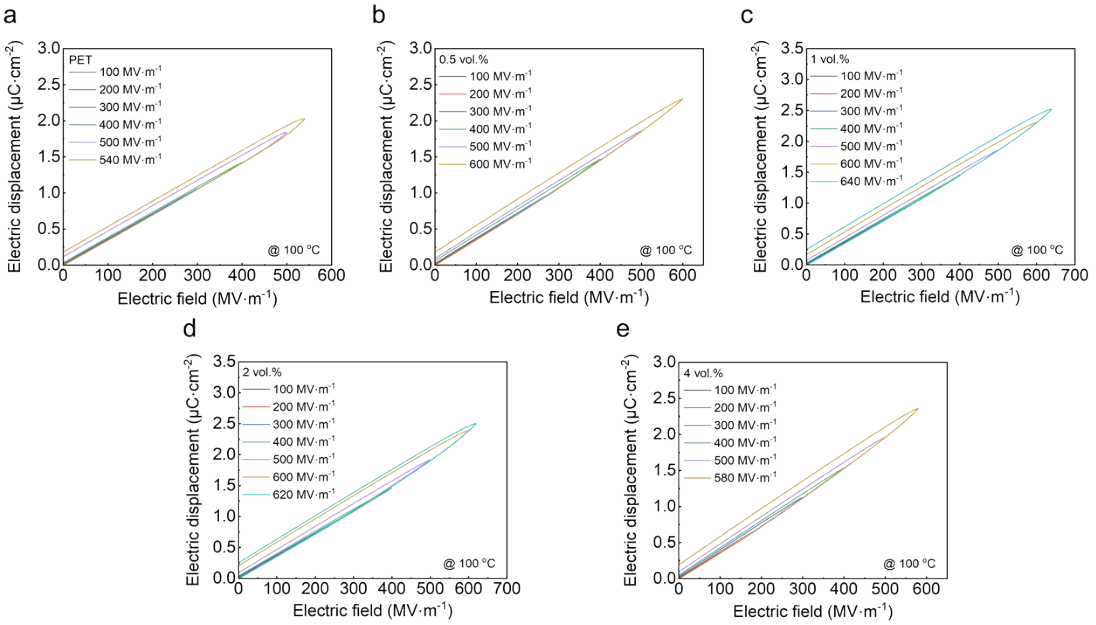

Figure S5. D-E hysteresis loops of PET and PET-S films at 100 °C under different electric field strengths.

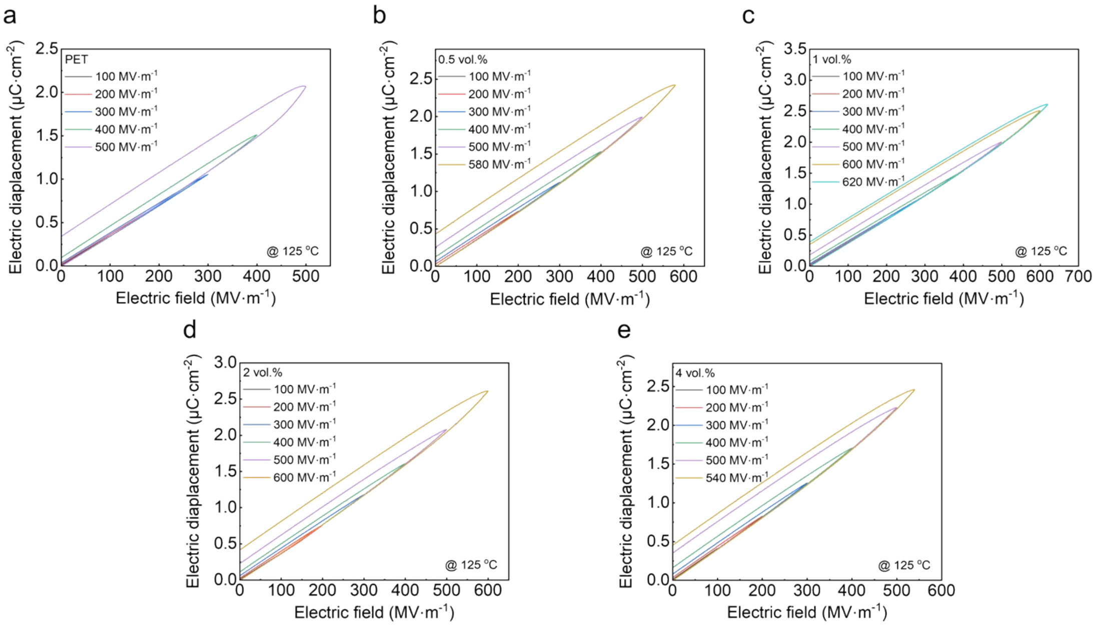

Figure S6. D-E hysteresis loops of PET and PET-S films at 125 °C under different electric field strengths.

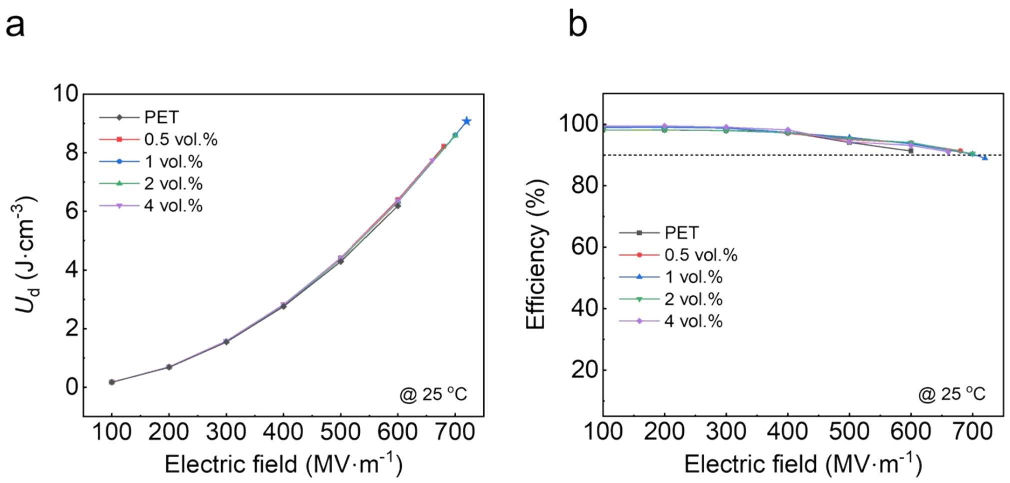

Figure S7. U_d and η of PET and PET-S films at 25 °C: (a) U_d. (b) η.

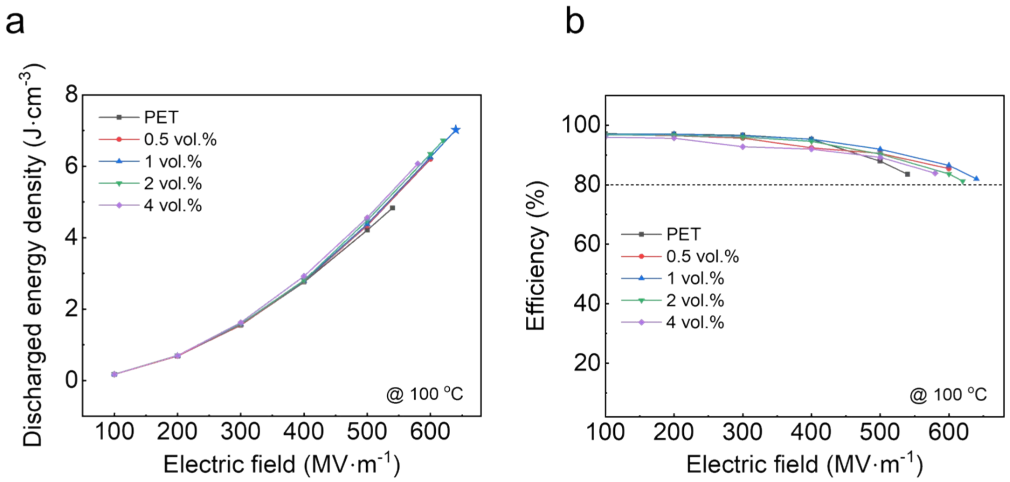

Figure S8. U_d and charge-discharge efficiency of PET and PET-S films at 100 °C: (a) U_d. (b) η.

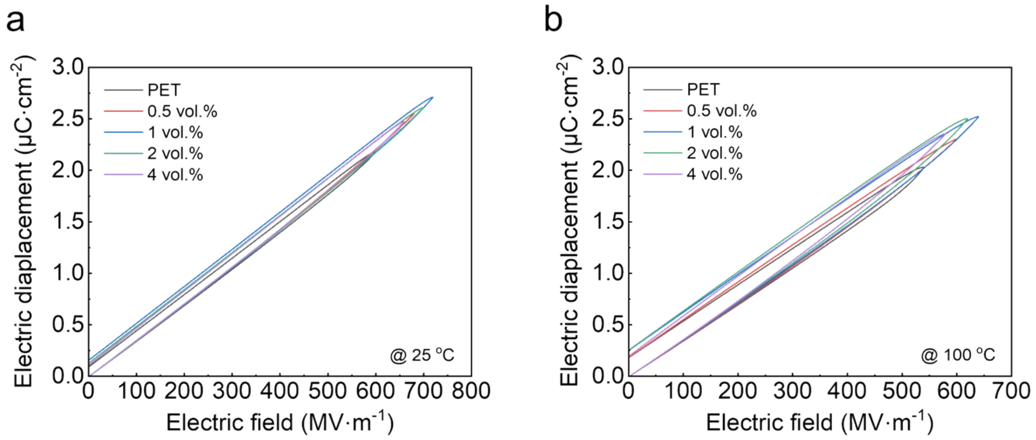

Figure S9. D-E hysteresis loops of PET and PET-S films at different temperatures: (a) 25 °C; (b) 100 °C.

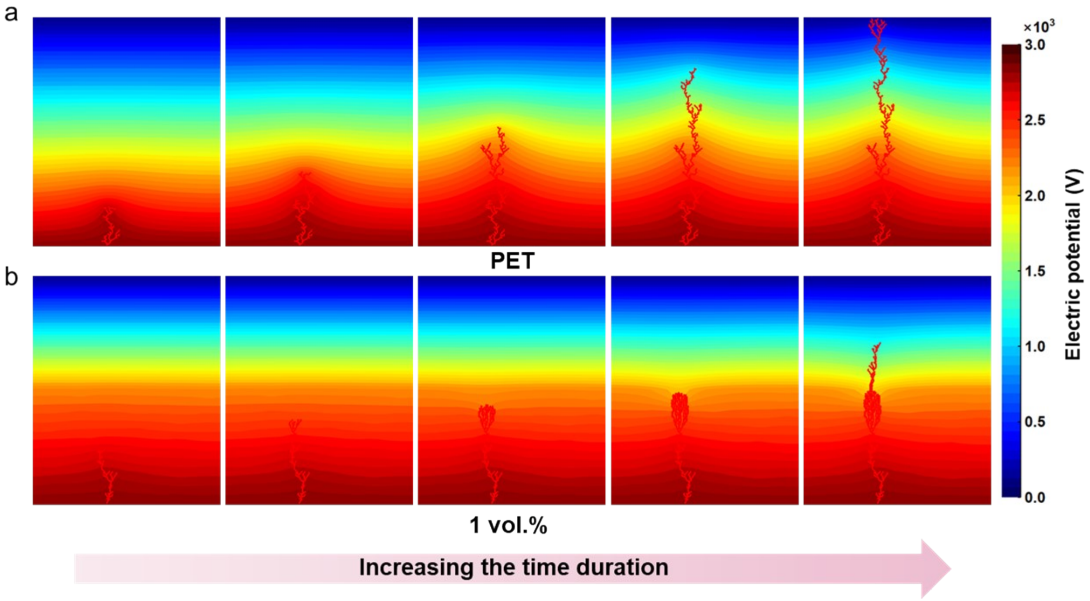

Figure S10. Electric potential and electrical branch evolution. (a) PET, (b) PET-S (1 vol.%).

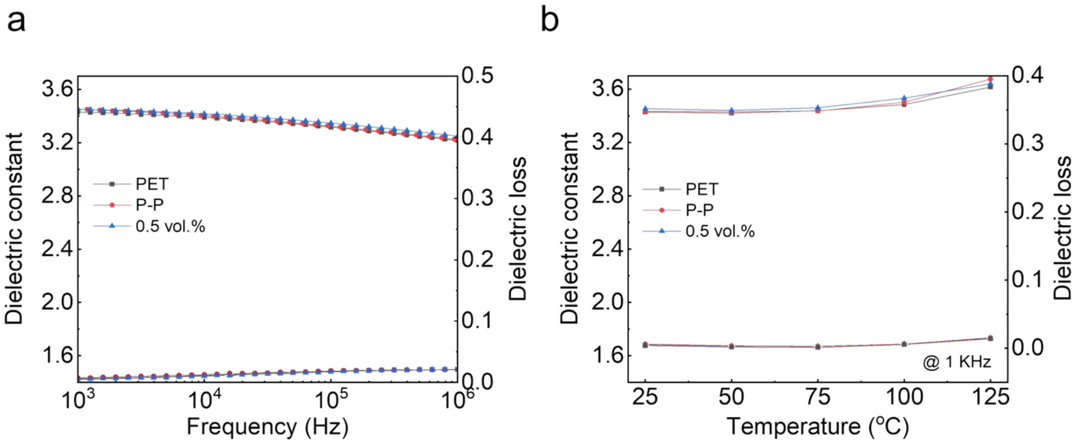

Figure S11. Dielectric properties of PET-P(VDF-HFP) (P-P) films: (a) Dielectric frequency spectrum; (b) Dielectric temperature spectrum (@1 kHz).

Figure S11a presents the ε_r of the polymer dielectric film PP at room temperature. Within the frequency range of 10^3-10^6 Hz, the ε_r of the P-P composite film increases compared to PET. At 1 kHz, it rises from 3.43 for pure PET to 3.45, with the limited increase primarily constrained by the thickness of the coating layer. Figure S11b illustrates the temperature dependence of the dielectric constant of the P-P film, which follows a trend similar to that of the PET film. This behavior is mainly attributed to the increased molecular chain mobility of PET at elevated temperatures, leading to variations in the dielectric constant.

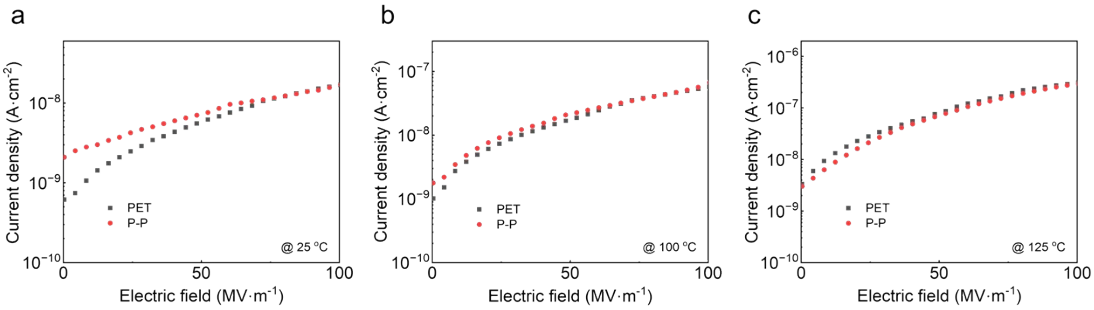

Figure S12. Variation of leakage current density with applied electric field for P-P films at different temperatures: (a) 25 °C. (b) 100 °C.

Figure S12 illustrates the variation in leakage current density of the P-P polymer film as a function of the electric field at different temperatures. As observed, the leakage current density of the P-P polymer film exhibits a trend nearly identical to that of the PET film. Moreover, the leakage current density does not decrease after coating the PET surface with P(VDF-HFP), indicating that the P(VDF-HFP) coating alone has a limited effect on improving the insulating properties of the PET film.

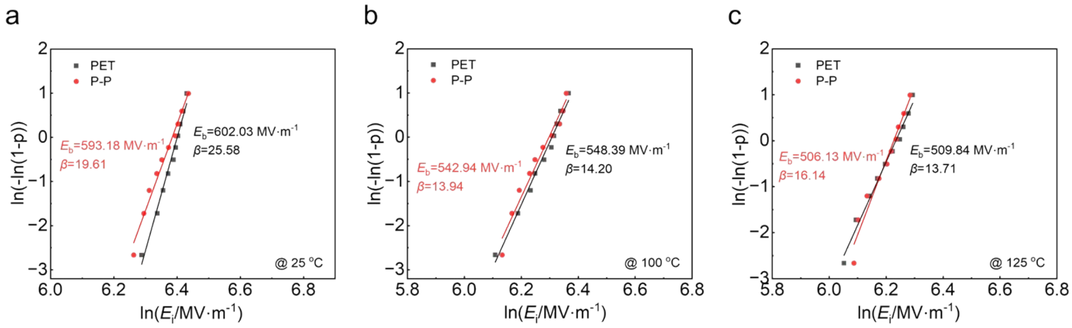

Figure S13. Weibull distribution of PET and P-P films at different temperatures: (a) 25 °C; (b) 100 °C; (c) 125 °C.

Figure S13 compares the breakdown strength of P-P polymer film and PET film at different temperatures. As shown, the breakdown strength of the P-P polymer film is nearly identical to that of the PET film, which is consistent with the results observed in Figure S12.

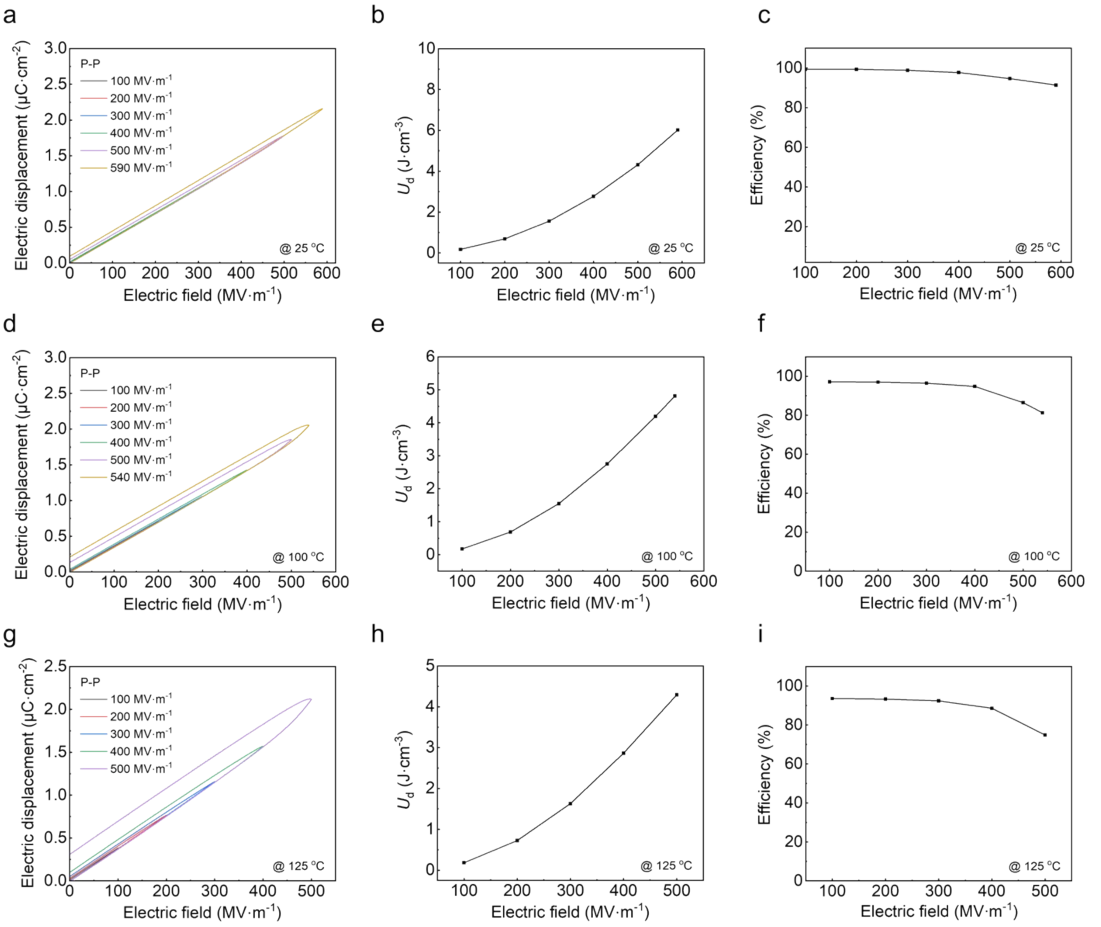

Figure S14. D-E hysteresis loops, U_d, and η of P-P films at different temperatures and electric field strengths: (a) D-E loop at 25 °C; (b) U_d at 25 °C; (c) η at 25 °C; (d) D-E loop at 100 °C; (e) U_d at 100 °C; (f) η at 100 °C; (g) D-E loop at 125 °C; (h) U_d at 125 °C; (i) η at 125 °C.

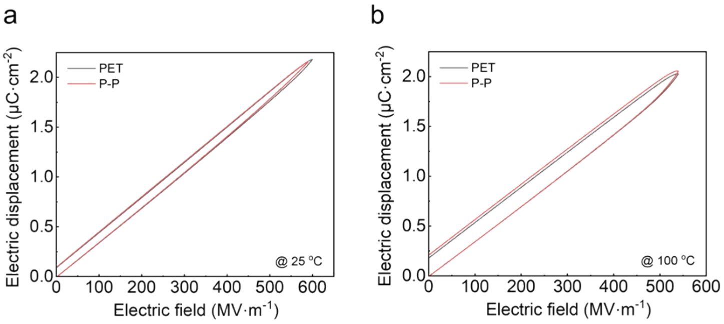

Figure S15. D-E hysteresis loops of PET and P-P films at different temperatures: (a) 25 °C; (b) 100 °C; (c) 125 °C.

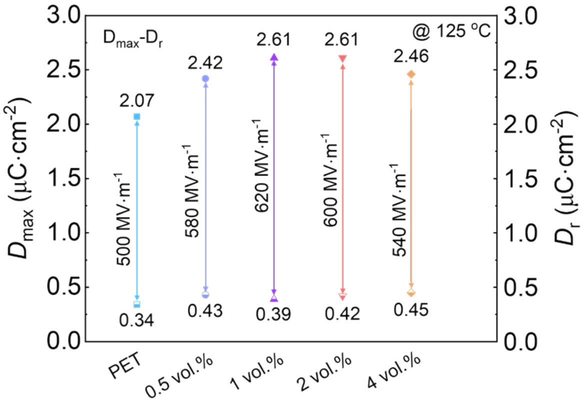

Figure S16. D_{max} and D_r of the composite films under the maximum electric field.